Supporting Information for

A General Strategy for Fabricating Isolated Single Metal Atomic Sites Catalysts in Y Zeolite

Yiwei Liu[†Δ], Zhi Li[†Δ], Qiuying Yu[‡], Yanfei Chen[§], Ziwei Chai[//], Guofeng Zhao[⊥], Shoujie Liu[#], Weng-Chon Cheong[†], Yuan Pan[†], Qinghua Zhang[¶], Lin Gu[¶], Lirong Zheng[£], Yu Wang[Θ], Yong Lu[⊥], Dingsheng Wang[†], Chen Chen[†], Qing Peng[†], Yunqi Liu[§], Limin Liu[//], Jiesheng Chen[*‡], and Yadong Li[*†]

[†] Department of Chemistry, Tsinghua University, Beijing 100084, China

[‡] School of Chemistry and Chemical Engineering, Shanghai Jiao Tong University, Shanghai 200240, China

[§] State Key Laboratory of Heavy Oil Processing, Key Laboratory of Catalysis, China University of Petroleum, Qingdao, Shandong 266580, China

[ǁ] Beijing Computational Science Research Center, Beijing 100193, China

[⊥] School of Chemistry and Molecular Engineering, East China Normal University, Shanghai 200062, China

[#] College of Chemistry and Materials Science, Anhui Normal University, Wuhu, Anhui 241000, China

[¶] Institute of Physics, Chinese Academy of Sciences, Beijing 100190, China

[£] Beijing Synchrotron Radiation Facility, Institute of High Energy Physics, Chinese Academy of Sciences, Beijing 100049, China

[Θ] Shanghai Synchrotron Radiation Facility, Shanghai Institute of Applied Physics, Chinese Academy of Sciences, Shanghai 201800, China

Experimental Procedures

Chemicals: $PtCl_2$, $PdCl_2$, 40 wt% colloidal silica (Alfa Aesar), $RuCl_3$, $RhCl_3 \cdot 3H_2O$ (Acros), NaOH, $NaAlO_2$, $CuCl_2 \cdot 2H_2O$, $CoCl_2 \cdot 6H_2O$, $NiCl_2 \cdot 6H_2O$ (Sinopharm Chemical), ethylenediamine, NH_4Cl, ammonium hydroxide (Beijing Chemical Reagent), were purchased and used without any further purification. Deionized water was used throughout.

Characterization: Transmission electron microscopy (TEM) images were taken on a Hitachi HT7700 transmission electron microscope. The high-resolution TEM, HAADF-STEM images, and the corresponding energy-dispersive X-ray (EDX) mapping were recorded by a JEOL JEM-2100F high resolution transmission electron microscope operating at 200 kV. Aberration-corrected HAADF-STEM images are taken on a JEOL JEM-ARM200F TEM/STEM with a spherical aberration corrector working at 300 kV. Inductively coupled plasma optical emission spectroscopy (ICP-OES) was measured by Thermo Fisher IRIS Intrepid II. Nitrogen adsorption and desorption isotherms were obtained at 77K using a Quantachrome Autosorb-1 instrument surface area analyzer. Powder X-ray diffraction patterns were measured with a Bruker D8 with Cu Kα radiation (λ =1.5406 Å). The in situ Fourier transform infrared (FTIR) spectra of CO adsorption were measured with a Nicolet 380/ZDF-X-LED in situ infrared spectrometer. The CO pulse chemisorptions were carried out on AutoChem II 2920 automated catalyst characterization system with a TCD detector.

Syntheses of zeolite NaY: NaOH, $NaAlO_2$, and H_2O were mixed and stirred until the solution is clear. Then 40 wt% colloidal silica and directing agent was dropwise added to the solution consecutively. After a continuous stirring for 4 hours and aged for 4 hours at room temperture. The reaction mixture was then transferred into a Teflon-lined stainless steel autoclave and the crystallization was conducted in a conventional oven at 100 °C for 12 hours. The final molar composition of the starting gel is 3.36 Na_2O: 1.0 Al_2O_3: 8.4 SiO_2: 250 H_2O. The as-synthesized solid products were centrifuged, washed with water and ethanol for several times, and then dried at 80 °C in the vacuum oven overnight.

Syntheses of zeolite HY: 1g zeolite NaY was suspended in 1.5 M NH_4Cl aqueous solution under continuous stirring at 80 ^oC for 6 hours. This process is repeated for three times. Then the solid products were centrifuged, washed with water and dried at 80 °C in the vacuum oven overnight. Then the obtained NH_4^+ form Y zeolite is calcined in static air at 400 ^oC for 2 hours to prepare HY zeolite.

Syntheses of Pt NPs@Y: Pt NPs@NaY was synthesized by the approaches reported previously with some modification.[1] Platinum was introduced as the tetra-ammine ion complex from queous solutions of the chloride to give desired loading of Pt (~ 0.23 wt%). A given mass of NaY zeolite (according to the content of Pt) was added into the solution as support. The suspension was stirred for 12 h at room temperature. The precipitates were separated by centrifugation and washed with water for five times followed by reduction in flowing H_2 (5%) at 600 ^oC for 1 hour. The Pt content was kept consistent with Pt-ISAS@Y by controlling the inventory and determined by ICP-OES. Pt NPs@HY was synthesized by the similar process, just the NaY zeolite was replaced by HY zeolite.

XAFS measurements: The X-ray absorption find structure spectra data were collected at 1W1B station in Beijing Synchrotron Radiation Facility (BSRF, operated at 2.5 GeV with a maximum current of 250 mA, Pt L3-edge, Co K-edge, Ni K-edge, Cu K-edge) and BL14W1 station in Shanghai Synchrotron Radiation Facility (SSRF, operated at 3.5 GeV with a maximum current of 250 mA, Pd K-edge, Ru K-edge and Ru K-edge), respectively. The XAFS data of M-ISASs samples were collected at room temperature in fluorescence excitation mode using a Lytle detector and all the references (metal foils and oxide bulks) were recorded in transmission mode using ionization chamber. All samples were pelletized as disks of 13 mm diameter with 1mm thickness using graphite powder as a binder.

EXAFS analysis: The acquired EXAFS data were processed according to the standard procedures using the ATHENA module implemented in the IFEFFIT software packages. The EXAFS spectra were obtained by subtracting the post-edge background from the overall absorption and then normalizing with respect to the edge jump step. Then, $\chi(k)$ data in the k-space were Fourier transformed to real (R) space using hanning windows (dk = 1.0 $Å^{-1}$) to separate the EXAFS contributions from different coordination shells. The quantitative information can be obtained by the least-squares curve fitting in the R space with a Fourier transform k space, using the module ARTEMIS of programs of IFEFFIT. The backscattering amplitude F(k) and phase shift $\Phi(k)$ were calculated using FEFF8.0 code..

Computational methods: DFT calculations were performed with the CP2K/Quickstep package,[2] which uses a hybrid Gaussian and plane-waves approach. For the exchange-correlation, we apply the Perdew-Burke-Ernzerhof (PBE) functional.[3] The vdW correction is considered with the Grimme approach (DFT-D3).[4] Core electrons were described with norm-conserving Goedecker, Teter, and Hutter (GTH) pseudopotentials.[5] Hydrogen was described by a TZVP-MOLOPT-GTH basis set, whereas all other atom types used DZVP-MOLOPT-SR-GTH.[6] For the auxiliary basis set of plane waves a 320 Ry cutoff was used. Reciprocal space sampling was restricted to the Γ point. The adopted convergence thresholds for the geometry optimizations were 10^{-4} Ha $Bohr^{-1}$ on the maximum atomic force, and 3×10^{-4} Ha $Bohr^{-1}$ on the root mean square residual of all the atomic forces. Calculations were all performed using periodic boundary conditions. The faujasite zeolite was modeled by a periodic cubic cell (a=b=c=24.35 angstrom), which contains the 192 units of SiO_2. Part of Si atoms are replaced by Al atoms according to the Si/Al ratio (2.5:1) from the experimental results. The nano platinum surface slab consisted of 5×5×3 (width, breadth and thickness, respectively.) platinum unit cells (>11.5 Å vacuum-buffer perpendicularly to the platinum 111 surface.). For single platinum stom, many possible adsorption sites for Pt in different cages were considered, and the most stable site is the Pt staying at the crosspoint of two connecting lines of two particular sets of oxygen atoms in the six member ring (Figure 2e). In order to understand the interaction between the Pt and the zeolite skeleton, the corresponding Lowdin charges were calculated for both the pure and doped Y zeolite model. As for the pure Y zeolite model, the charge transfer between the model and Pt is 0.06 e, which indicates the interaction between the Pt and the skeleton is rather weak. While for the doped model, the charge transfer becomes

0.13 e, thus the Pt atom bonds more strongly with the Si-O-Al sites. Transition states along the reaction pathways are searched by the constraint method.

References

(1) L. Xu, X.-C. Xu, L. Ouyang, X.-J. Yang, W. Mao, J. Su, Y.-F. Han, Mechanistic study of preferential CO oxidation on a Pt/NaY zeolite catalyst. *J. Catal.* **2012,** *287*, 114-123.

(2) J. VandeVondele, M. Krack, F. Mohamed, M. Parrinello, T. Chassaing, J. Hutter, Quickstep: Fast and accurate density functional calculations using a mixed Gaussian and plane waves approach. *J. Comput. Phys. Commun.* **2005,** *167*, 103-128.

(3) J. P. Perdew, K. Burke, M. Ernzerhof, Generalized Gradient Approximation Made Simple. *Phys. Rev. Lett.* **1996,** *77*, 3865-3868.

(4) S. Grimme, J. Antony, S. Ehrlich, H. Krieg, A consistent and accurate ab initio parametrization of density functional dispersion correction (DFT-D) for the 94 elements H-Pu. *J. Chem. Phys.* **2010,** *132*, 154104.

(5) S. Goedecker, M. Teter, J. Hutter, Separable dual-space Gaussian pseudopotentials. *Phys. Rev. B* **1996,** *54*, 1703-1710.

(6) J. VandeVondele, J. Hutter, Gaussian basis sets for accurate calculations on molecular systems in gas and condensed phases. *J. Chem. Phys.* **2007,** *127*, 114105.

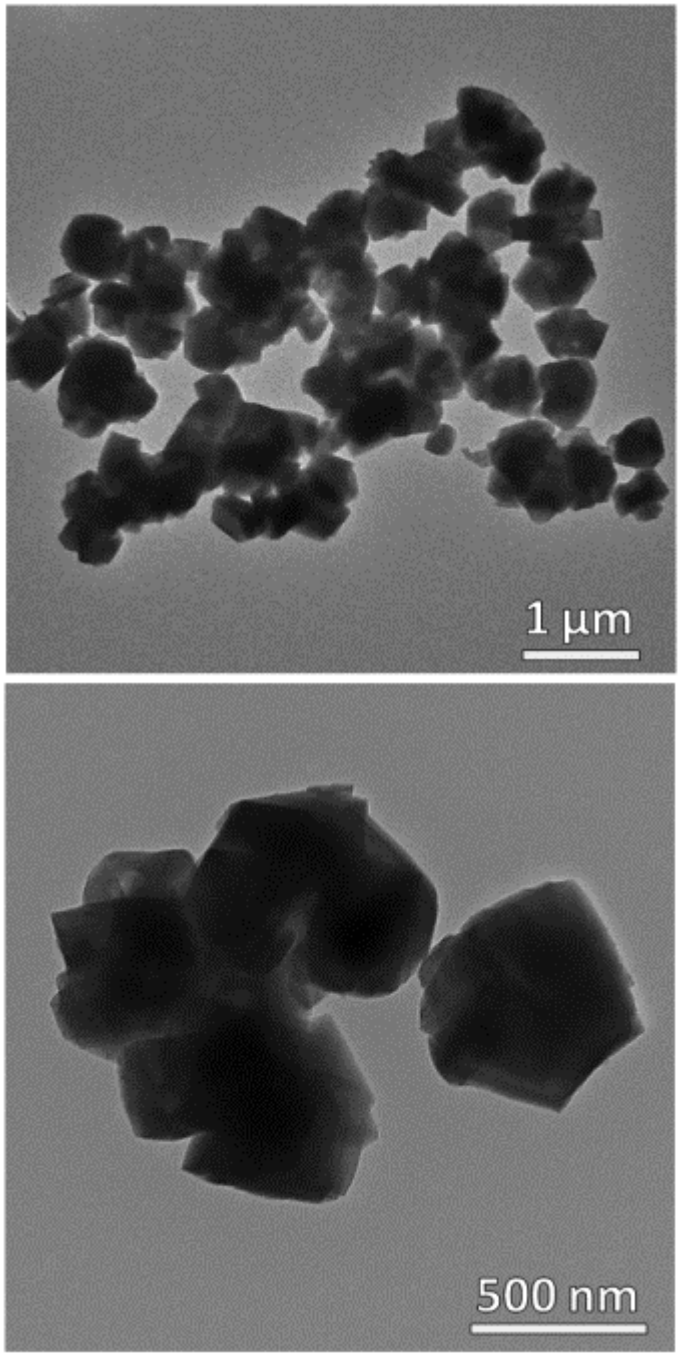

Figure S1. TEM images of Pt-EDA@NaY with different magnification.

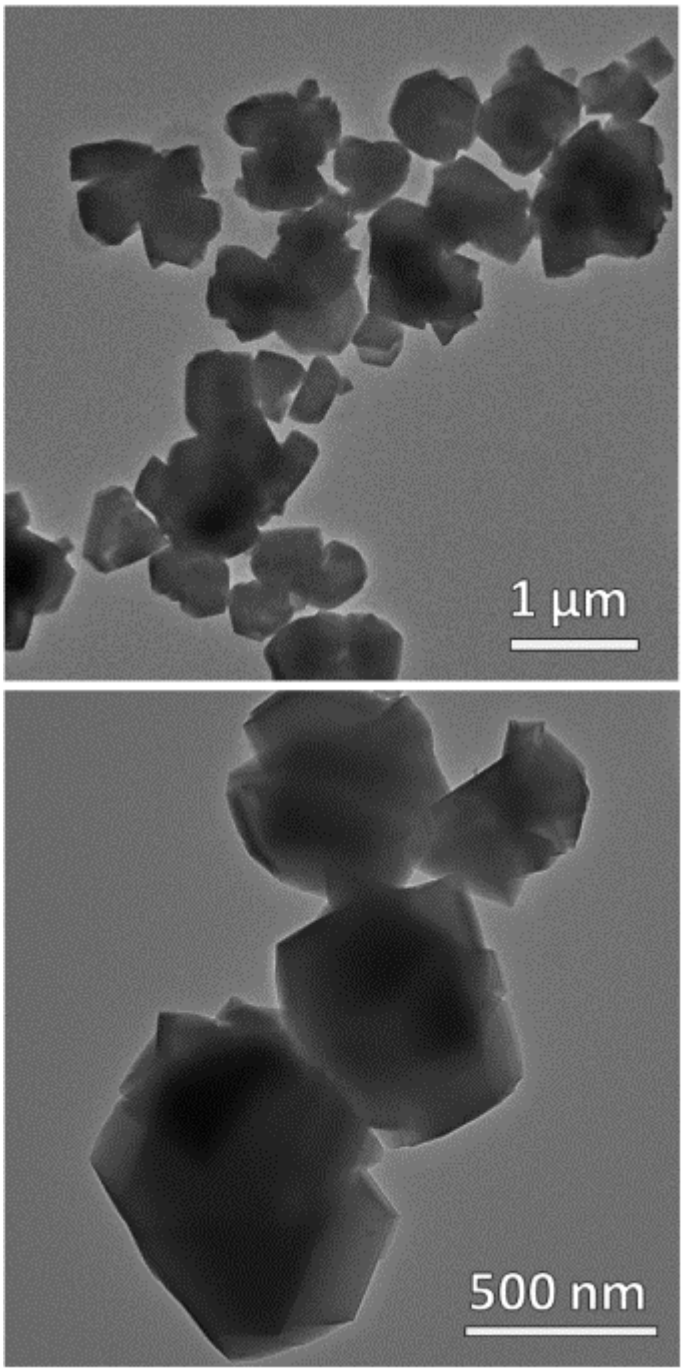

Figure S2. TEM images of Pt-ISAS@NaY with different magnification.

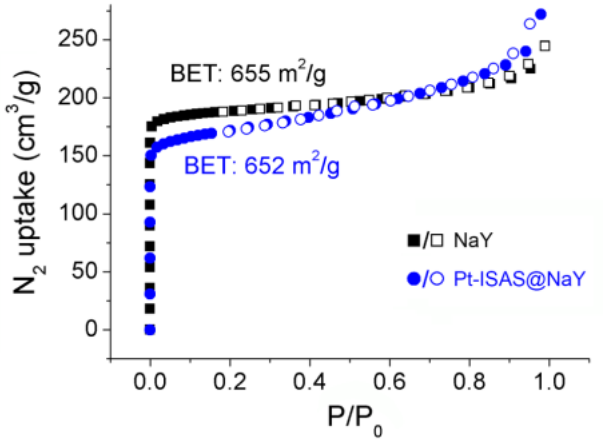

Figure S3. N_2 adsorption/desorption isotherm of NaY and Pt-ISAS@NaY repectively.

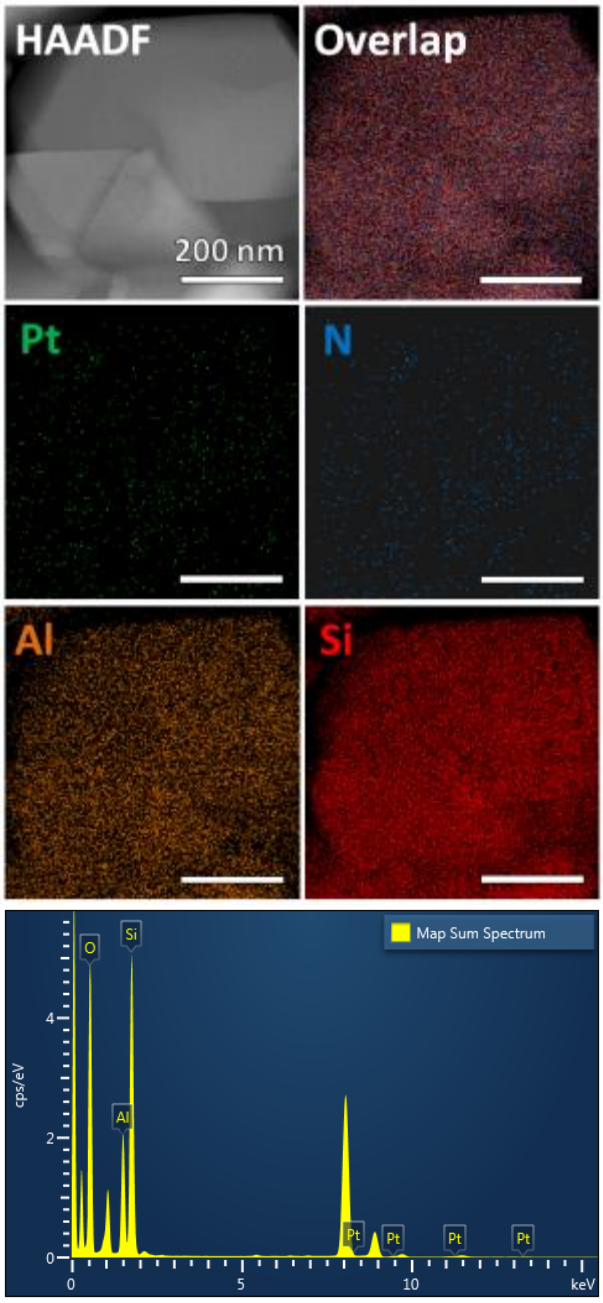

Figure S4. HAADF image, element mapping spectra and corresponding energy dispersive X-ray analysis of Pt-EDA@NaY.

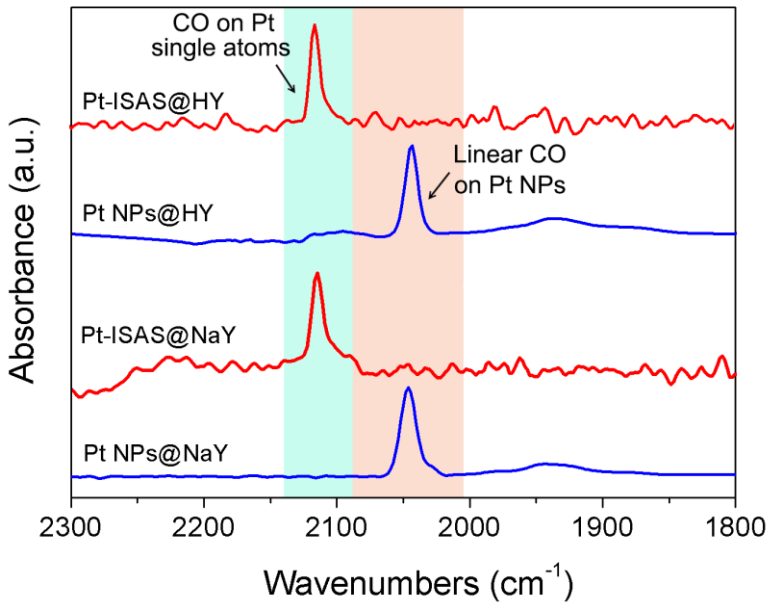

Figure S5. In situ FTIR spectra of CO adsorption for different Pt species on Y zeolite. The band at 2116 cm^{-1} is ascribed to CO linearly adsorbed on $Pt^{\delta+}$, and the band at 2047 cm^{-1} is ascribed to CO linearly adsorbed on Pt NPs.

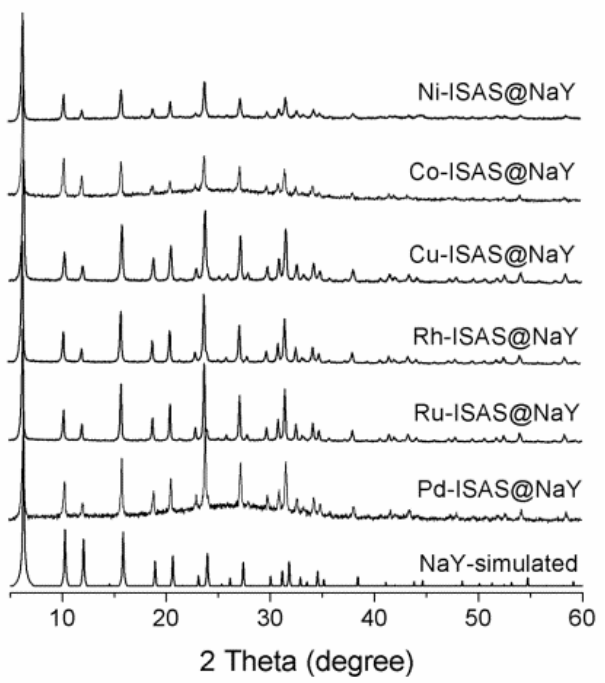

Figure S6. PXRD of NaY-simulated, Pd-ISAS@NaY, Ru-ISAS@NaY, Rh-ISAS@NaY Cu-ISAS@NaY, Co-ISAS@NaY, and Ni-ISAS@NaY respectively.

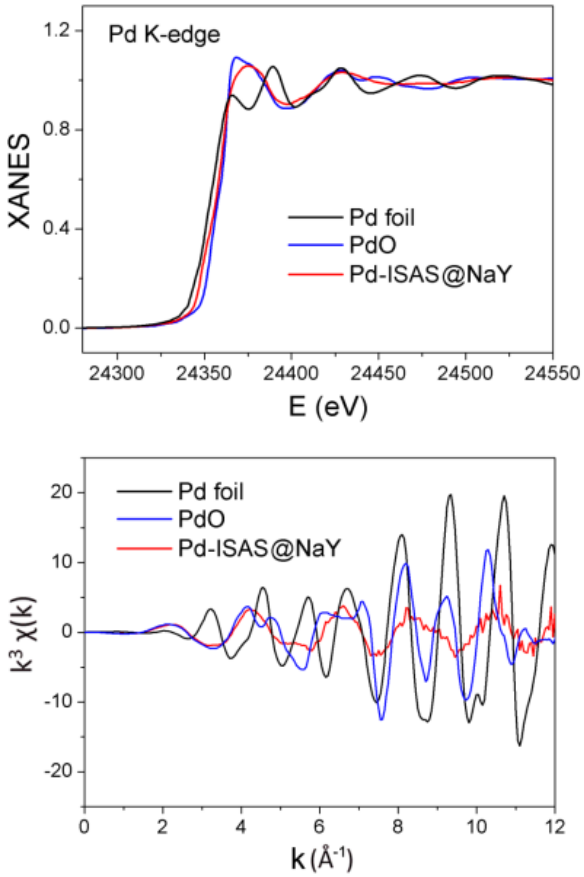

Figure S7. XANES of Pd K-edge for Pd-ISAS@NaY with reference materials Pd foil and PdO.

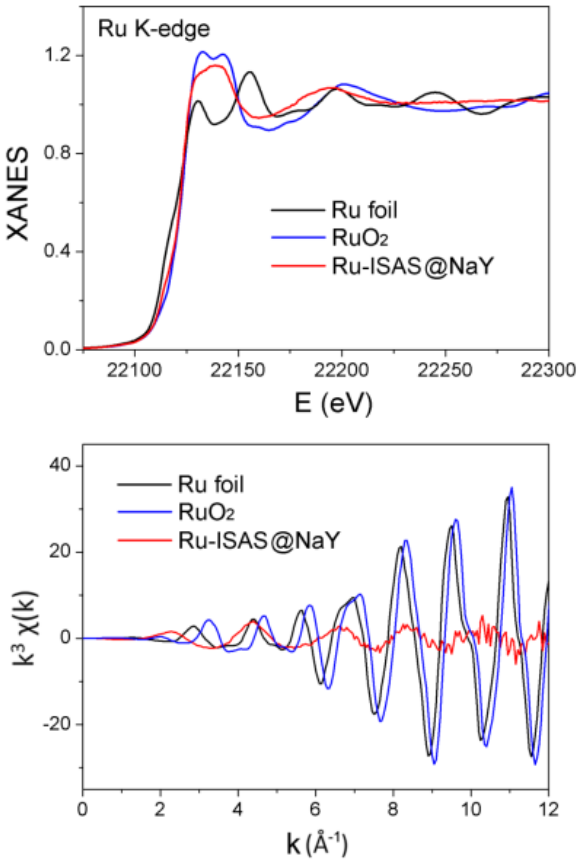

Figure S8. XANES of Ru K-edge for Ru-ISAS@NaY with reference materials Ru foil and RuO_2.

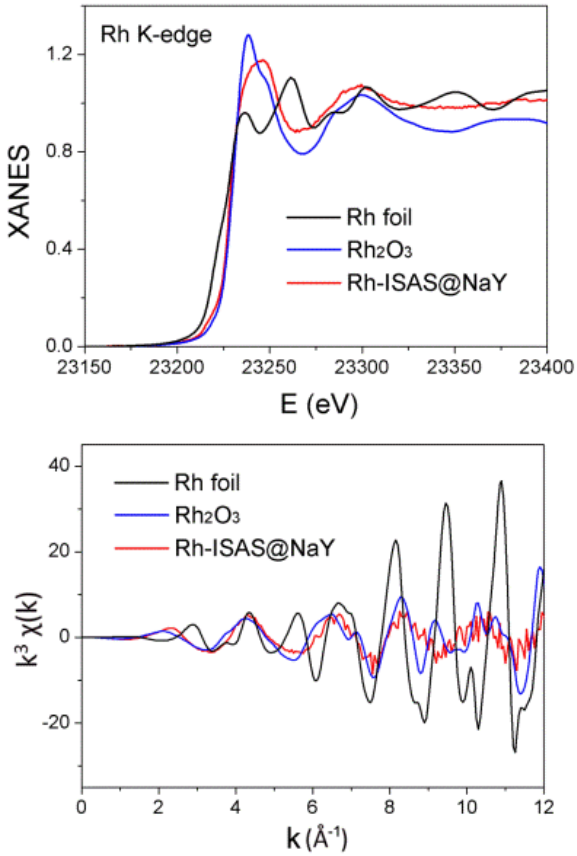

Figure S9. XANES of Rh K-edge for Rh-ISAS@NaY with reference materials Rh foil and Rh_2O_3.

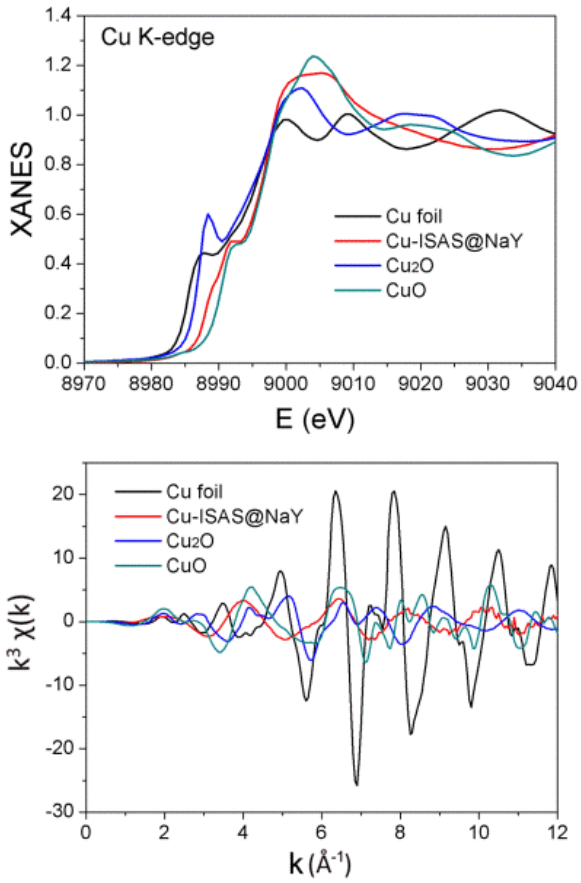

Figure S10. XANES of Cu K-edge for Cu-ISAS@NaY with reference materials Cu foil, Cu_2O, and CuO.

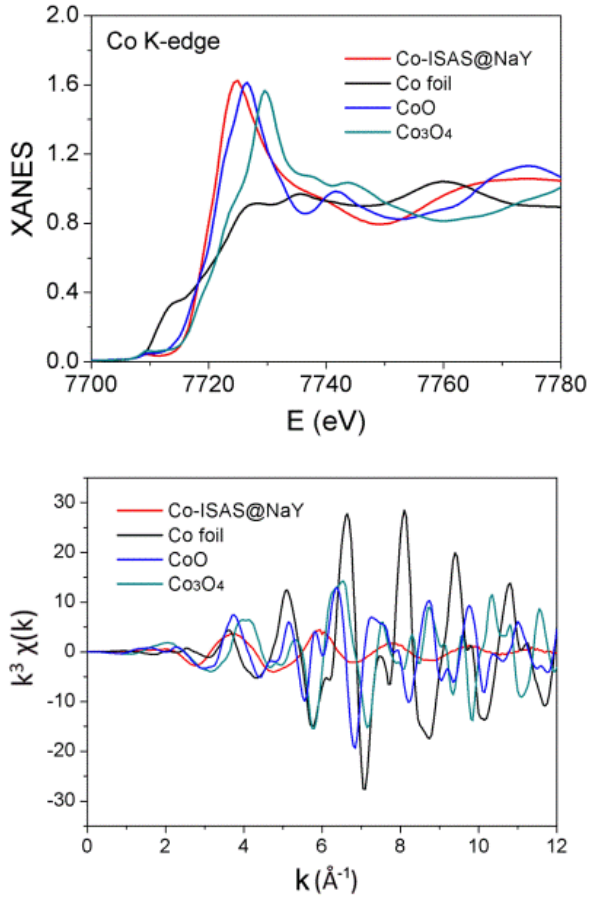

Figure S11. XANES of Co K-edge for Co-ISAS@NaY with reference materials Co foil, CoO and Co_3O_4.

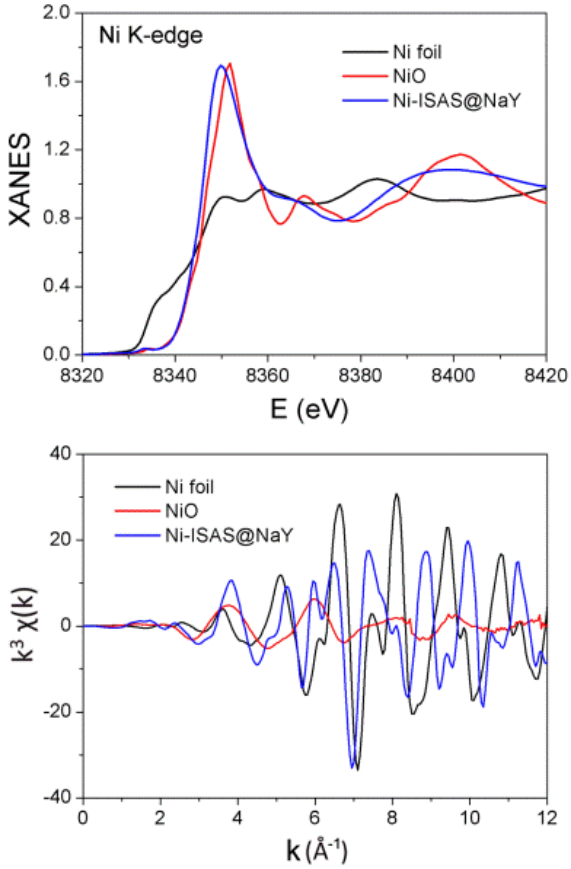

Figure S12. XANES of Ni K-edge for Ni-ISAS@NaY with reference materials Ni foil and NiO.

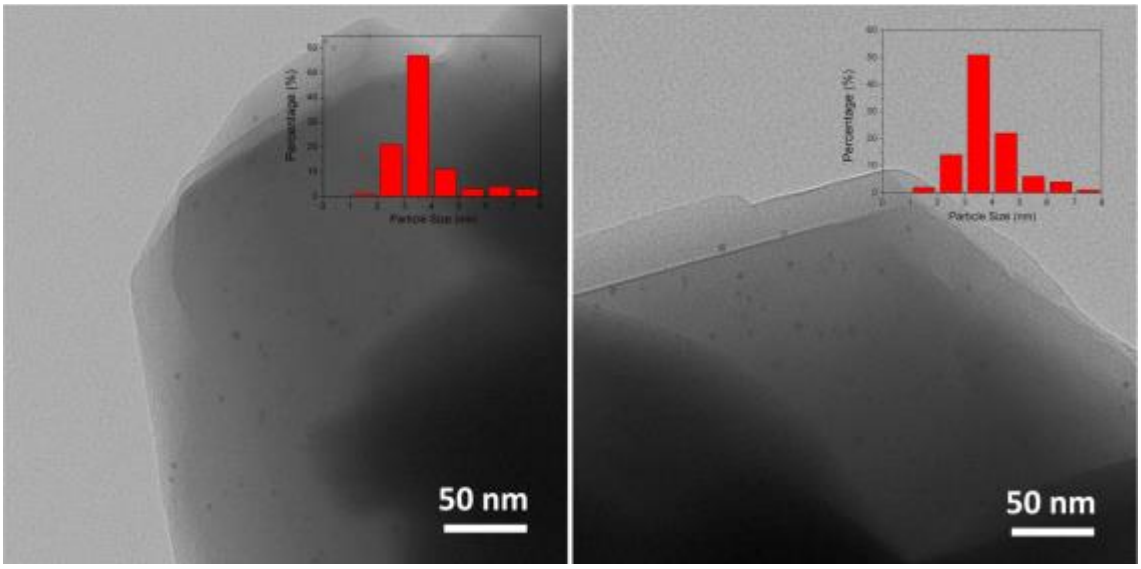

Figure S13. TEM images and particle size distribution of Pt NPs@NaY (left) and Pt NPs@HY (right), the average particle size is about 3.5 nm, and the morphology is sphere.

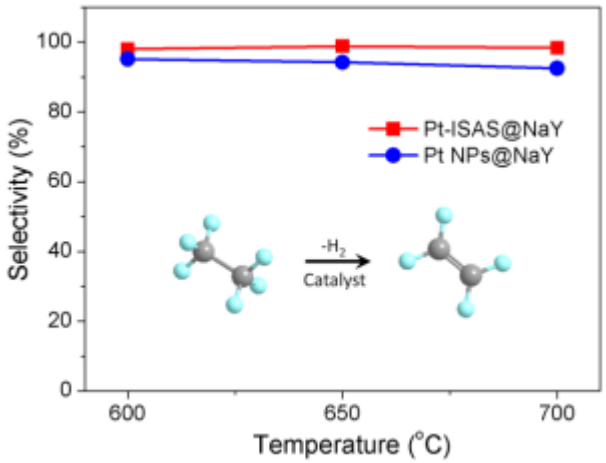

Figure S14. The selectivity of ethane dehydrogenation use Pt-ISAS@NaY and Pt NPs@NaY as catalysts repectively.

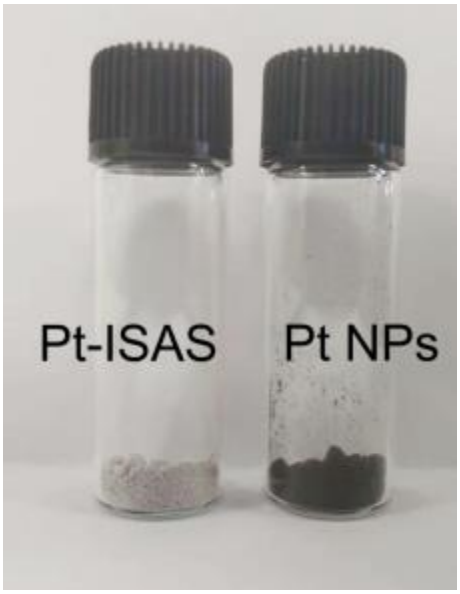

Figure S15. The recovered catalysts after ethane dehydrogenation.

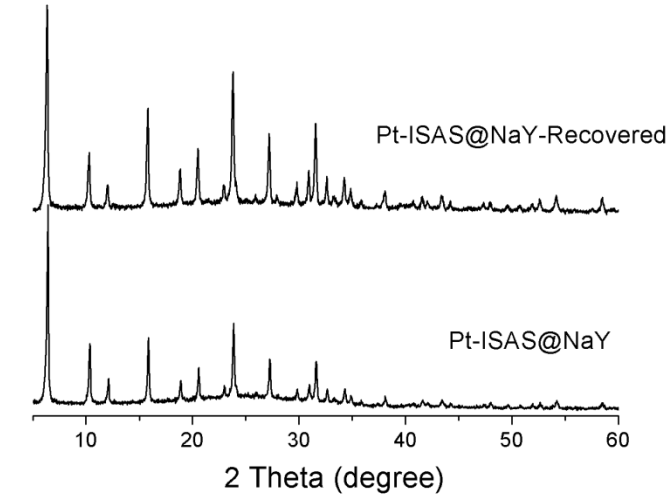

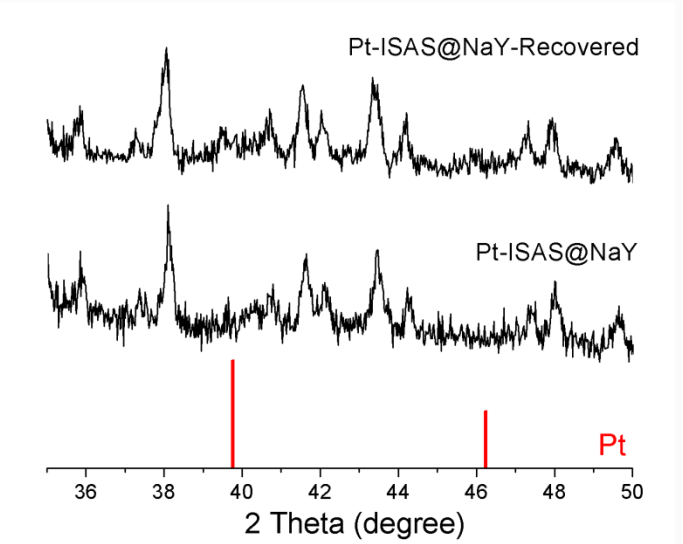

Figure S16. PXRD of fresh Pt-ISAS@NaY and recovered Pt-ISAS@NaY after used for ethane dehydrogenation.

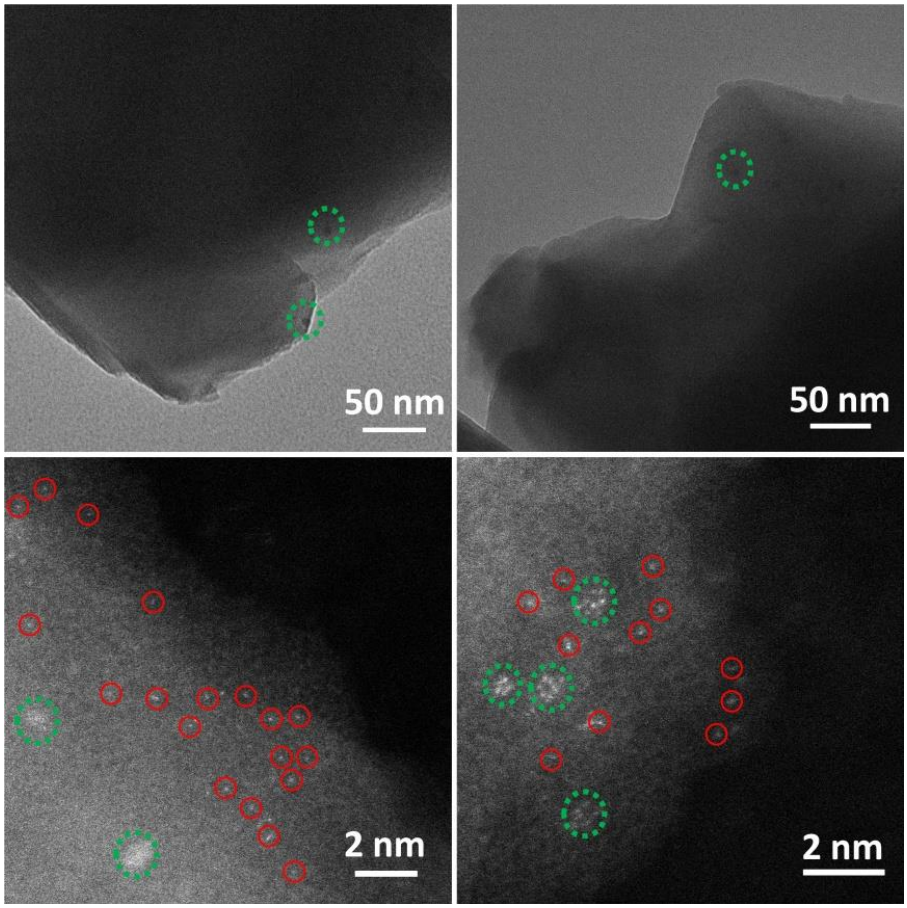

Figure S17. TEM images and AC-HAADF-STEM images of recovered Pt-ISAS@**Na**Y.

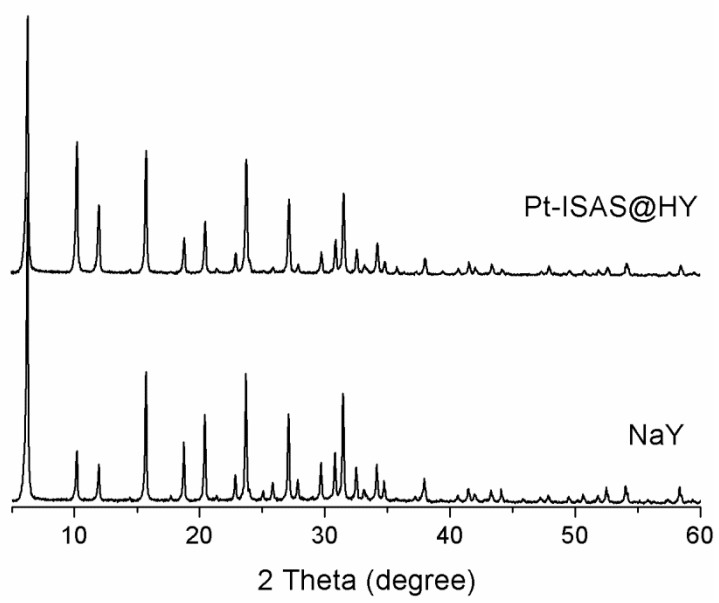

Figure S18. PXRD of NaY and Pt-ISAS@HY.

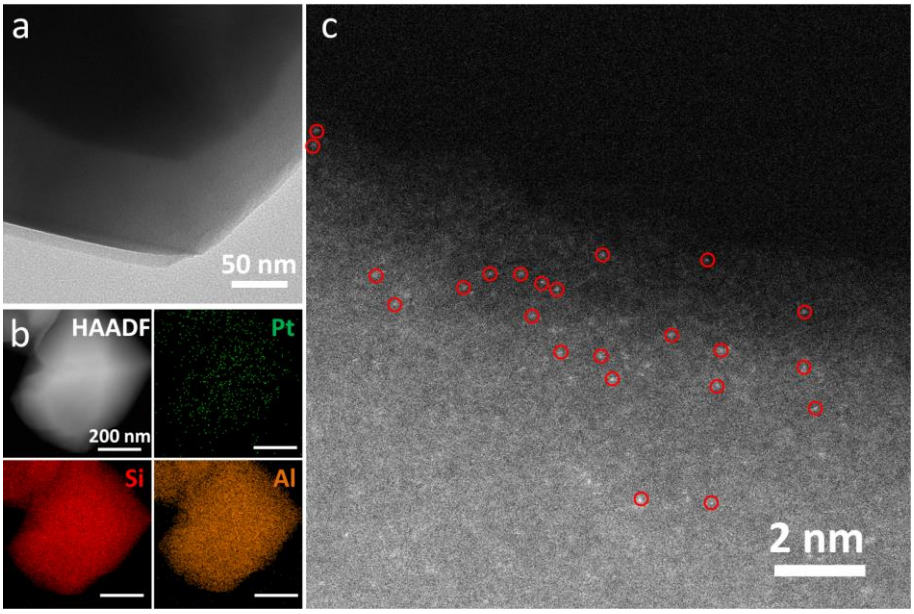

Figure S19. (a) TEM image, (b) elements mapping, and (c) AC-HAADF-STEM image of Pt-ISAS@HY.

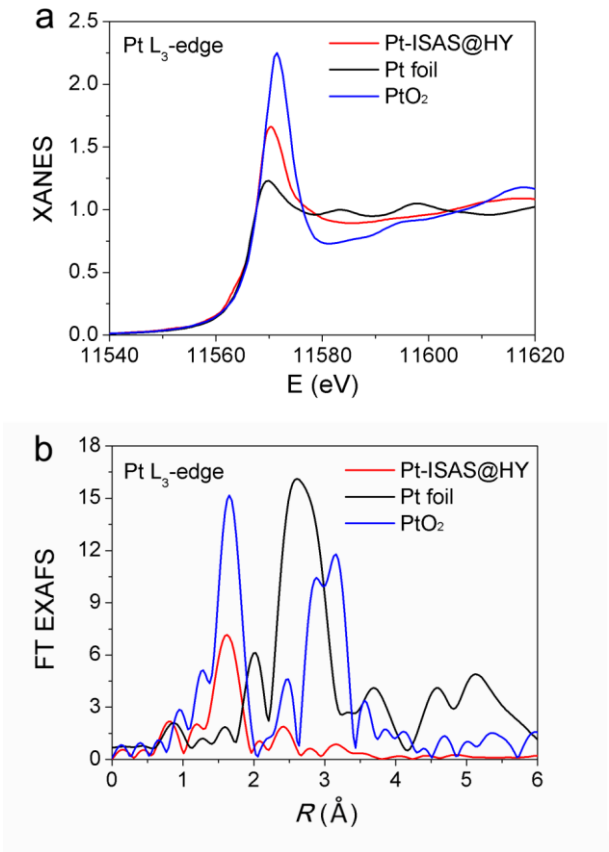

Figure S20. (a) XANES of Pt L_3-edge for Pt-ISAS@HY with reference materials Pt foil and PtO_2. (b) Fourier transforms of k^3-weighted Pt L_3-edge EXAFS experimental data for Pt foil, Pt-ISAS@HY, and PtO_2.

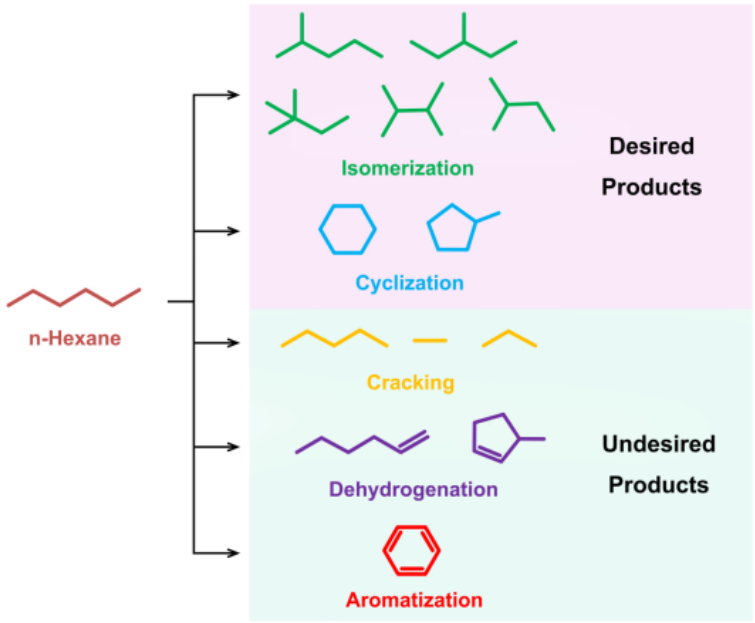

Figure S21. The possible products in the catalytic reforming of n-hexane. Isomerization and cyclization products are desired, while dehydrogenation, aromatization, and cracking are undesired.

Table S1. Pt dispersion determined by CO chemsorption measurements at 323K

Sample	Pt content (wt%)	Size	Dispersion ($mol_{active\ sites}/mol_{Pt}$%)
Pt-ISAS@NaY	0.22	Single atom	99.51%
Pt-ISAS@HY	0.22	Single atom	98.53%
Pt NPs@NaY	0.23	3.5 nm	39.46%
Pt NPs@HY	0.23	3.5 nm	40.17%

The active site number and dispersion were calculated assuming a stoichiometry of one CO molecule per accessible Pt atom. Prior to CO chemsorption, the fresh samples were treated at 473K for 60 min and then cooled to 323K under a argon flow (40 ml/min).

Table S2. Structural parameters of **Pt-ISAS@NaY** extracted from the EXAFS fitting. (S_0^2=0.85)

Scattering pair	CN	R(Å)	σ^2(10^{-3}Å^2)	ΔE_0(eV)	R factor
Pt-O	2.3±0.4	2.01±0.02	8.67±1.7	4.6±1.4	0.0074

S_0^2 is the amplitude reduction factor; CN is the coordination number; R is interatomic distance (the bond length between central atoms and surrounding coordination atoms); σ^2 is Debye-Waller factor (a measure of thermal and static disorder in absorber-scatterer distances); ΔE_0 is edge-energy shift (the difference between the zero kinetic energy value of the sample and that of the theoretical model). R factor is used to value the goodness of the fitting.

Table S3. The metal concentration of different M-ISAS@Y from ICP results.

Element	Pt	Pd	Ru	Rh	Co	Ni	Cu
Metal Concentration (wt%)	0.22	0.56	0.22	0.09	0.65	0.31	0.29

Table S4. Comparison of the activity and selectivity of *n*- hexane hydroisomerization between Pt-ISAS@HY, Pt NPs@HY and other catalysts reported in the literatures.

Catalyst	T (℃)	P (bar)	Selectivity	Mass activity (mol g^{-1} s^{-1})	TOF_{Pt} (h^{-1})
Pt-ISAS@HY (0.22%)	**340**	**1 bar**	**98.1 %**	**2.25 E^{-6}**	**717**
Pt NPs@HY (0.23%)	**340**	**1 bar**	**96%**	**0.45 E^{-6}**	**142**
Pt-ISAS@NaY (0.22%)	**340**	**1 bar**	**80%**	**1.49 E^{-8}**	**4.7**
HY	**340**	**1 bar**	**-**	**4 E^{-8}**	**-**
NaY	**340**	**1 bar**	**-**	**None**	**-**
Pt@Al-MCF-17 (0.25%)[1]	360	1 bar	85 %	0.22 E^{-6}	61
Pt@Al-MCF-17 (0.5%)[1]	360	1 bar	92 %	1.32 E^{-6}	184
Pt@Al-MCF-17 (1%)[1]	360	1 bar	93 %	1.25 E^{-6}	86
PTA⊂MIL-101/Pt (0.1%)[2]	250	1 bar	93 %	6.8 E^{-8}	47
Pt@Nb_2O_5 (0.6%) [3]	360	1 bar	97.9 %	-	79
Pt@Ta_2O_5 (0.6%) [3]	360	1 bar	97.2 %	-	86
Pt@Al-MCF-17 (0.5%)[4]	360	1 bar	> 90 %	-	425
Pt-ISAS@m-Al_2O_3 (0.2%)[5]	550	1 bar	50 %	1.77 E^{-7}	61
Pt@TiO_2 (0.65%)[6]	440	1 bar	53 %	2 E^{-6}	220
Pt/CsPW (0.32%)[7]	180	1 bar	-	-	44
0.28%Pt/0.35%Au/CsPW[7]	180	1 bar	-	-	96

(1) Musselwhite, N.; Na, K.; Sabyrov, K.; Alayoglu, S.; Somorjai, G. A., Mesoporous Aluminosilicate Catalysts for the Selective Isomerization of *n*-Hexane: The Roles of Surface Acidity and Platinum Metal, *J. Am. Chem. Soc.* **2015**, 137, 10231−10237

(2) Sabyrov, K.; Jiang, J.; Yaghi, O. M.; Somorjai, G. A., Hydroisomerization of *n*-Hexane Using Acidified Metal-Organic Framework and Platinum Nanoparticles. *J. Am. Chem. Soc.* **2017**, 139, 12382–12385

(3) An, K.; Alayoglu, S.; Musselwhite, N.; Na, K.; Somorjai, G. A., Designed catalysts from Pt nanoparticles supported on macroporous oxides for selective isomerization of *n*-hexane. *J. Am. Chem. Soc.* **2014**, 136, 6830−6833

(4) Musselwhite, N.; Na, K.; Alayoglu, S.; Somorjai, G. A., The pathway to total isomer selectivity: *n*-hexane conversion (reforming) on platinum nanoparticles supported on aluminum modified mesoporous silica (MCF-17). *J. Am. Chem. Soc.* **2014**, 136, 16661−16665

(5) Zhang, Z.; Zhu, Y.; Asakura, H.; Zhang, B.; Zhang, J.; Zhou, M.; Han, Y.; Tanaka, T.; Wang, A.; Zhang, T.; Yan, N., Thermally stable single atom Pt/m-Al_2O_3 for selective hydrogenation and CO oxidation. *Nat. Comm.* **2017**, 10.1038/ncomms16100

(6) An, K.; Zhang, Q.; Alayoglu, S.; Musselwhite, N.; Shin, J. Y.; Somorjai, G. A., High-temperature catalytic reforming of n-hexane over supported and core-shell Pt nanoparticle catalysts: role of oxide-metal interface and thermal stability. *Nano Lett.* **2014**, 14, 4907−4912
(7) Alazman, A.; Belic, D.; Kozhevnikova, E. F.; Kozhevnikov, I. V., Isomerisation of n-hexane over bifunctional Pt-heteropoly acid catalyst: Enhancing effect of gold. *J. Catal.* **2018**, 357, 80–89